

The ROMS IAS Data Assimilation and Prediction System: Quantifying Uncertainty

Andrew M. Moore

Department of Ocean Sciences, 1156 High St.

University of California

Santa Cruz CA 95064

Phone: (831) 459-4632 fax: (831) 459-4882 email: ammoore@ucsc.edu

Brian Powell

Department of Oceanography

University of Hawai'i at Manoa

1000 Pope Road

Honolulu HI 96822

Phone: (808) 956-6724 fax: (808) 956-2352 email: powellb@hawaii.edu

Award Number: N00014-08-1-0556

LONG-TERM GOALS

The long-term scientific goals of this research project are:

1. To develop a state-of-the-art ocean 4-dimensional variational (4D-Var) data assimilation and ocean forecasting system for the Regional Ocean Modeling System (ROMS);
2. To develop a state-of-the-art suite of post-processing and diagnostic tools in support of ROMS 4D-Var;
3. To gain the necessary experience using the ROMS 4D-Var systems in complex circulation environments;
4. To train the next generation of users of the ROMS 4D-Var system.

OBJECTIVES

The main objectives of this project are: (i) to assess the impact of observations on ocean state estimates and the ensuing forecasts; (ii) to quantify the expected errors in 4D-Var ocean circulation estimates; and (iii) to develop multimodel ensemble and superensemble methods for ocean models.

APPROACH

DISTRIBUTION STATEMENT A.

The primary tool used is the Regional Ocean Modeling System (ROMS) and the Terrain-coordinate Ocean Modeling System (TOMS). To address the aforementioned goals and objectives, we are using a recently developed suite of tools that utilize the tangent linear (TL), adjoint (AD), and finite-amplitude tangent linear (RP) versions of the ROMS/TOMS code.

Report Documentation Page				Form Approved OMB No. 0704-0188	
Public reporting burden for the collection of information is estimated to average 1 hour per response, including the time for reviewing instructions, searching existing data sources, gathering and maintaining the data needed, and completing and reviewing the collection of information. Send comments regarding this burden estimate or any other aspect of this collection of information, including suggestions for reducing this burden, to Washington Headquarters Services, Directorate for Information Operations and Reports, 1215 Jefferson Davis Highway, Suite 1204, Arlington VA 22202-4302. Respondents should be aware that notwithstanding any other provision of law, no person shall be subject to a penalty for failing to comply with a collection of information if it does not display a currently valid OMB control number.					
1. REPORT DATE 2009		2. REPORT TYPE		3. DATES COVERED 00-00-2009 to 00-00-2009	
4. TITLE AND SUBTITLE The ROMS IAS Data Assimilation and Prediction System: Quantifying Uncertainty				5a. CONTRACT NUMBER	
				5b. GRANT NUMBER	
				5c. PROGRAM ELEMENT NUMBER	
6. AUTHOR(S)				5d. PROJECT NUMBER	
				5e. TASK NUMBER	
				5f. WORK UNIT NUMBER	
7. PERFORMING ORGANIZATION NAME(S) AND ADDRESS(ES) University of California ,Department of Ocean Sciences,1156 High St,Santa Cruz,CA,95064				8. PERFORMING ORGANIZATION REPORT NUMBER	
9. SPONSORING/MONITORING AGENCY NAME(S) AND ADDRESS(ES)				10. SPONSOR/MONITOR'S ACRONYM(S)	
				11. SPONSOR/MONITOR'S REPORT NUMBER(S)	
12. DISTRIBUTION/AVAILABILITY STATEMENT Approved for public release; distribution unlimited					
13. SUPPLEMENTARY NOTES					
14. ABSTRACT					
15. SUBJECT TERMS					
16. SECURITY CLASSIFICATION OF:			17. LIMITATION OF ABSTRACT Same as Report (SAR)	18. NUMBER OF PAGES 15	19a. NAME OF RESPONSIBLE PERSON
a. REPORT unclassified	b. ABSTRACT unclassified	c. THIS PAGE unclassified			

ROMS, TLROMS and ADROMS were developed under the support of previous ONR funding, while the development of RPROMS was supported by NSF. Three 4D-Var data assimilation systems have been configured for ROMS (Moore et al., 2009a,b): one which searches for ocean circulation estimates in the full space spanned by the model, and two which search for circulation estimates that are linear combinations of the observed model variables. The former is referred to as a model- or primal-space search, and the algorithm used in ROMS is based on the incremental formulation used in numerical weather prediction (NWP), and here after referred to as I4D-Var (Courtier et al., 1994). The latter systems search in observation- or dual-space, and the algorithms used in ROMS are the Physical-space Statistical Analysis System (4D-PSAS) (Da Silva et al., 1995) and an indirect representer method (R4D-Var) (Egbert et al., 1994).

The ROMS I4D-Var algorithm has been used extensively in a number of different geographical regions (e.g. Intra-Americas Sea, California Current, East Australia Current, Indonesian Seas, New Jersey Bight), and the ROMS user community is gaining much needed experience in applying sophisticated 4D-Var methods in mesoscale coastal circulation environments (Di Lorenzo et al., 2007; Haidvogel et al., 2008; Muccino et al., 2008; Powell et al., 2008, 2009; Broquet et al., 2009a,b,c; Zhang et al., 2009a,b). ROMS I4D-Var has been also been used in a real-time assimilation and prediction mode in the Intra-Americas Sea (Powell et al., 2009). The advent of 4D-PSAS and R4D-Var however is more recent, and our experience with these algorithms is so far limited to the California Current system and the Intra Americas Sea (IAS).

The utility of ROMS 4D-Var has increased considerably during the last 6 months. In addition to the three 4D-Var systems that are now online, users can now augment the control vector for any application to include adjustments to the initial conditions, surface forcing and open boundaries, as well as increments that account for model error. Also, an improved specification of the multi-variate prior/background error covariance matrices is available.

The current project builds on the previous efforts with the specific goals of developing three new and important capabilities for ROMS. These are: (i) development of new drivers for ROMS that provide information about the efficacy of the ocean circulation estimates derived from ROMS 4D-Var; (ii) development of the adjoint of the ROMS 4D-Var algorithms to provide information about the impact of each assimilated observation on the resulting circulation estimates, and the sensitivity of these estimates to changes in the observations themselves; and (iii) development of a methodology for multi-model ensemble analysis and prediction. We will report here on the progress to date in each of these three sub-projects.

WORK COMPLETED

During the current reporting period we have completed the following tasks:

1. **Expected analysis error:** Drivers have been configured for ROMS that allow some members of the EOF spectrum of the expected posterior/analysis error covariance matrix (hereafter denoted \mathbf{E}^a) of resulting 4D-Var circulation estimates to be computed. For I4D-Var, only EOFs corresponding to the least significant analysis error EOFs can be readily computed owing to the search in model-space. However, experience in NWP suggests that these can provide useful information about likely analysis error patterns (Fisher and Courtier, 1995). Conversely, in the case of 4D-PSAS and R4D-Var the leading EOFs of the analysis error covariance can be readily computed by capitalizing on

the results of intermediate steps of the minimization procedure in observation/dual-space (Moore et al., 2009). Both options are now available in ROMS

In addition, the expected posterior/analysis error variance, the leading diagonal of \mathbf{E}^a , can be computed in the case of 4D-PSAS and R4D-Var. Both the EOF and analysis error variance calculations capitalize on the Lanczos formulation of the conjugate gradient algorithm that is used to minimize the 4D-Var cost function. The Lanczos vectors that are computed during each iteration of the 4D-Var algorithms can be used to build reduced rank estimates of both the diagonal of \mathbf{E}^a and the off-diagonal covariance information using the EOFs.

2. **Observation impact and sensitivity:** It is easy to show that the adjoint of the entire 4D-Var assimilation system provides valuable information about the impact of observations on the circulation estimate, as well as the sensitivity of the circulation to variations in the observations (Langland and Baker, 2004). The impact of each assimilated observation on any quantifiable aspect of the analysis and forecast increments can be readily computed by reconstructing the transpose of the approximate Kalman gain matrix for each assimilation cycle. This is readily achieved in ROMS using the Lanczos vectors of the 4D-Var minimization algorithms. This option is now available for I4D-Var, 4D-PSAS and R4D-Var in ROMS. On the otherhand, the change in any quantifiable aspect of the analysis increments and forecast errors due to a change in any assimilated observation can be computed using the adjoint of the entire 4D-Var cycle (Zhu and Gelaro, 2008). Such changes in the observations can include suppressing the influence of particular observations during the assimilation cycle, which may be used to circumvent costly observation system simulation experiments (OSSEs) and subsequent optimal observation array design. This option is currently available for 4D-PSAS and R4D-Var, but is impractical at the present time for I4D-Var. Efforts are also underway using the representer functions implicit within R4D-Var to quantify the efficacy of observation arrays by using antenna analysis and array modes (Bennett, 1985).
3. **Multimodel ensemble methods:** Initial efforts are underway to utilize a simple linear regression-based superensemble method developed in NWP by Krishnamurti et al. (2000). This work has been conducted by a 1st year Ocean Sciences graduate student, Ms. Jo Beck, at UC Santa Cruz under the direction of Andrew Moore. The methodology is being developed initially using an ensemble of ROMS IAS calculations driven by different fields of surface forcing and open boundary conditions. Once the method has been fully developed and tested, it will be applied to a multi-model ensemble comprised of different hindcast products from various ocean modeling centers, including ROMS.
4. **Improved ROMS configuration for the IAS:** Earlier versions of ROMS configured for the IAS were found to poorly reproduce the deep water masses of the region. This was subsequently found to be due to deficiencies in the open boundary conditions and the bathymetry being used. After a prolonged and extensive series of experiments by Powell, a new ROMS IAS configuration has been identified which is able to faithfully maintain the water mass properties throughout the water column and throughout the IAS region. Experiments are now underway using this recently developed ROMS IAS configuration, and some data assimilation results are presented below.

RESULTS

(a) Expected Analysis Error

For the period 2006-2007, we assimilated observations into ROMS IAS using I4D-Var, and computed estimates of the expected analysis errors to determine how each data type contributes to the reduction in the prior error. As part of the operational assimilation and prediction system that was developed under previous ONR funding, we relied upon real-time satellite data that had not benefited from the rigorous quality control of science-quality data. By examining the temporal evolution of the analysis error, we were able to determine whether real-time or delayed-time satellite products would provide a greater reduction in the uncertainty of the best estimate circulation. The results of this work are published in Powell and Moore (2009), and are summarized below.

One of the most surprising findings of the study was that significant differences exist between the real-time and post-processed satellite data. Figure 1 shows the rms at each grid point between the real-time and post-processed of SSH and SST. In SSH (SST) there is a mean rms of 9.7 cm (0.65°C), suggesting that the difference between observational products may often exceed the difference between observations and the best circulation estimate, creating significant challenges for real-time, operational data assimilation. Given the difference between the observational products, we are interested in how each data product impacts the best circulation estimate and the expected analysis error.

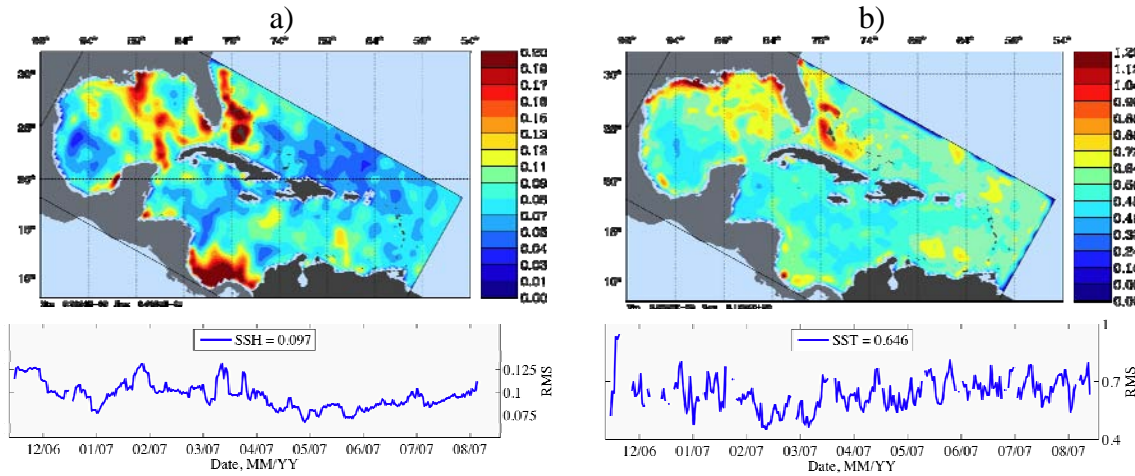


Figure 1: The rms difference between real-time and post-processed satellite products for (a) SSH, and (b) SST. Each map shows the point-wise rms over time, while the time-series shows the rms in space. SSH exhibits a mean rms difference of 9.7 cm, while SST shows a mean RMS difference of 0.65°C.

We performed four independent I4D-Var assimilation experiments using combinations of the real-time and post-processed SSH and SST data, and calculated the expected analysis error after each assimilation cycle. The mean temporal and spatial rms differences between the best circulation estimate and each observation type remained less than the rms difference between each observation (cf Fig. 1). Therefore, despite the large differences between satellite data products, the assimilation procedure was able to identify a circulation estimate that was more accurate than the uncertainties inherent in the satellite data sets themselves.

The expected analysis error reveals a number of interesting results. The trace of different blocks of both the *prior* (background) and expected *posterior* (analysis) error yields a useful scalar measure of the total error variance associated with each control variable. Time series of each trace estimate are shown in Fig. 2 for various experiments. The resulting analysis error trace for the SST block of \mathbf{E}^a (Fig. 2b) shows that as the assimilation cycles proceed, the *posterior* error continually decreases as the model circulation approaches the observed circulation. Surprisingly, SSH (Fig. 2a) displays no apparent reduction in analysis error. This does not mean that the assimilated SSH field did not improve. On the contrary, the assimilation of SSH reduces the rms difference between the model and observations by over 50%. However, as noted above, only the least significant EOFs of \mathbf{E}^a can be identified during I4D-Var explaining only a small fraction of the expected SSH error variance.

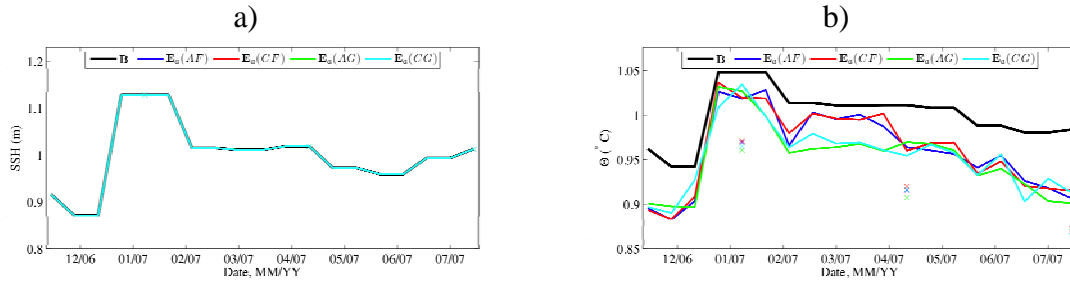


Figure: 2 Time series of the temporal evolution of the trace of different blocks of the prior/background error covariance matrix (black) and posterior/analysis error covariance matrix (separate colors for different experiments). The trace for the SSH block is shown in (a), while the trace for the temperature block is shown in (b). The period March-April where the AF and CF products have higher uncertainty illustrates the effect of data loss in the observational product.

Figure 2 indicates that the uncertainty in the entire temperature field has been reduced by assimilating only SST. Figure 3 shows a transect in the Gulf of Mexico and illustrates the reduction in analysis error resulting from assimilating the real-time product versus a post-processed SST. Surprisingly, the analysis error in the jet of the LC was reduced further by using the real-time product.

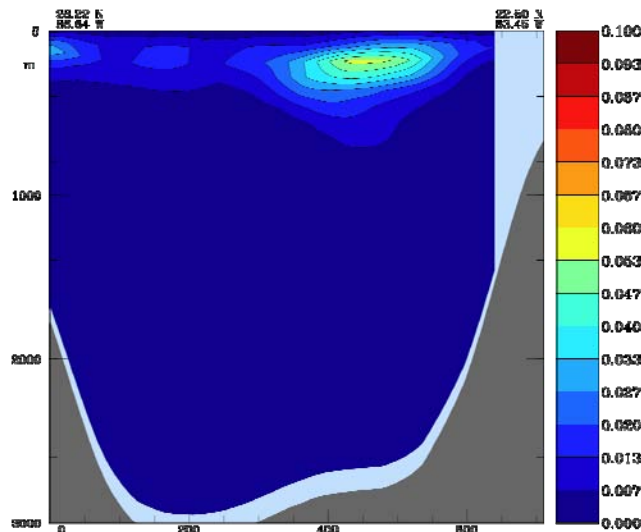


Figure 3: A transect across the Gulf of Mexico (Cuba to the right) showing the reduction in expected analysis error from assimilating the post-processed SST product versus the real-time product. The real-time SST has reduced the uncertainty in the core Loop Current north of Cuba more than the post-processed product.

Recent Advances in the Intra-Americas Sea

If 4D-Var is performed in dual-space instead using 4D-PSAS or R4D-Var, it is possible to compute an estimate of the full expected *posterior*/analysis error variance for each model state variable. This circumvents the problems mentioned above in primal-space where only the least significant EOFs of \mathbf{E}^a can be readily computed. Recent calculations using R4D-Var and the improved ROMS IAS configuration reveal the impact of satellite data on the *posterior*/analysis error.

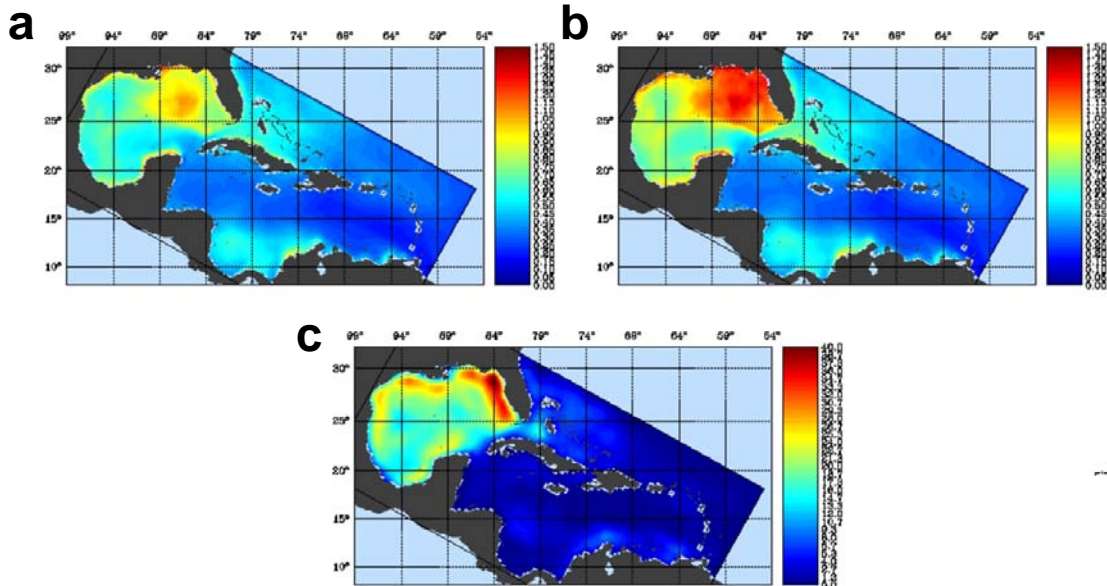


Figure 4: The annual average (a) *posterior* error variance, and (b) *prior* error variance in SST during 1999. (c) The percentage reduction on *prior* error in SST. In (a) and (b) the range plotted is 0-1.5 K^2 while in (c) the range plotted is 0-40%.

Figure 4 shows the annual average *prior* and expected *posterior* analysis error variance for SST from 1999 during which satellite SST and SSH were assimilated sequentially every 7 days into ROMS IAS using R4D-Var. A comparison of Figs. 4a and 4b reveals that R4D-Var has significantly reduced the expected analysis error variance in the Gulf of Mexico. Figure 4c shows the percentage reduction of the *posterior* error variance compared to the *prior* error variance for SST and reveals that the error reduction can be as large as 40% along the west coast of Florida.

The California Current System (CCS)

As noted above, the leading EOFs of \mathbf{E}^a are not readily accesible using I4D-Var because of the primal-space search for the best circulation estimate. However, if instead the search is performed in dual-space using 4D-PSAS or R4D-Var, the circulation estimate obtained is the same as in I4D-Var (Courtier, 1997) and the leading EOFs of \mathbf{E}^a can be computed at little extra computational cost (Moore et al., 2009a). Figure 4 shows an example of the cumulative explained variance by the first 200 EOFs of \mathbf{E}^a for a R4D-Var assimilation cycle in the California Current System (CCS). The dimension of \mathbf{E}^a is nominally $O(10^5)$ while Fig. 4 indicates that less than 0.1% of the EOF spectrum accounts for ~40% of the analysis error variance.

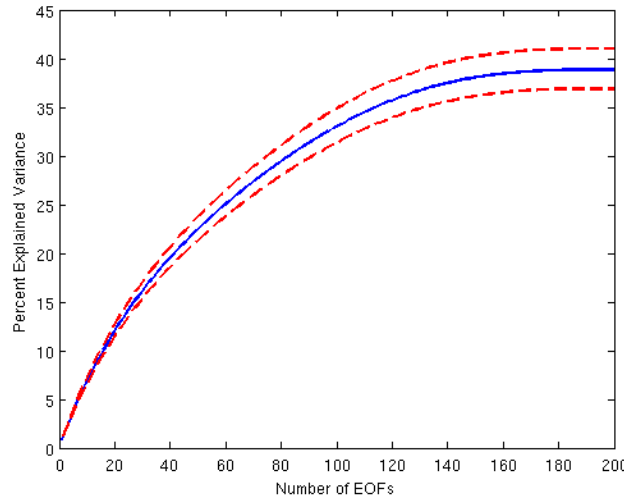


Figure 4: The cumulative percentage explained variance (blue curve) by the first 200 EOFs of the expected analysis error covariance matrix for a representative assimilation cycle in the California Current system. The red curves indicate the range of uncertainty associated with the estimate of the trace of \mathbf{E}^a .

(b) Observation Impact and Sensitivity

California Current System (CCS)

Much of the observation impact and observation sensitivity development work to date has been performed using ROMS configured for the CCS. This is due primarily to the excellent observation coverage along the U.S. west coast which has allowed us to more effectively test the new ROMS drivers and algorithms in the presence of several different sources of observational

data. A representative example observation impact calculation is shown in Fig. 5 which illustrates how various sources of observational information contribute to the CCS upper ocean transport in the analysis increments along 37N on one particular day of a given assimilation cycle during April 2003. During the 7 day assimilation cycle, a total ~16,000 observations were available from various platforms including: satellite SST, satellite SSH, hydrographic data from repeat cruise tracks as part of the CalCOFI and GLOBEC/LTOP programs, ARGO profiling floats, XBTs, and temperature observation collected by tagged California elephant seals as part of the Tagging of Pacific Pelagics program (TOPP). Figure 5 shows that while the lion's share of data are surface observations from satellites, the largest impact on the analysis increment transport at 37N (~63%) comes from the subsurface observations which constitute less than 10% of the total number of observations.

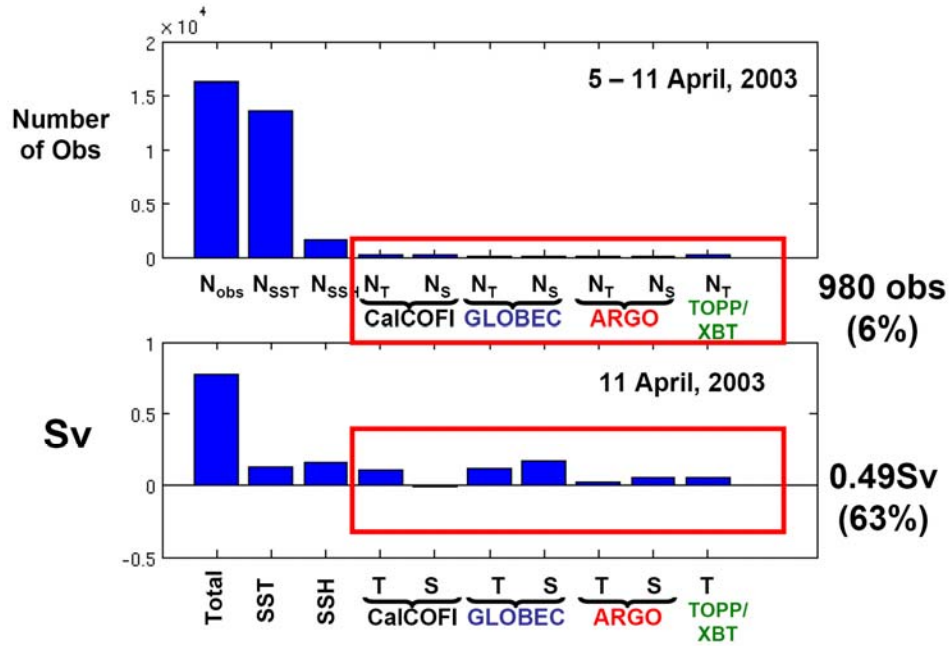


Figure 5: The lower panel shows the analysis increment CCS transport along 37N in the upper 500m on 11 April 2003 for a single 7 day assimilation cycle using R4D-Var ("Total"). The contribution of each observation type to the Total transport is also indicated: SST= satellite SST; SSH=satellite SSH; T=subsurface temperature; S=subsurface salinity. The transport explained by the subsurface data alone from CalCOFI, GLOBEC/LTOP, tagged elephant seals (TOPP) and XBTs is 0.49Sv, some 63% of the Total. The upper panel indicates the number of each type of observation assimilated during this cycle, and the total number of all observation, $N_{obs} \sim 1.6 \times 10^4$. The total number of subsurface T and S observations is 980, some 6% of the total, which account for 63% of the analysis increment CCS transport.

While Fig. 5 shows the aggregate impact of each observation type, the impact of each individual datum is also readily available as illustrated in Fig. 6 which shows the contribution to the analysis increment transport of (a) satellite SST on a single day, and (b) a single CTD cast collected along CalCOFI Line 90. The value and utility of this kind of information for routine observation monitoring and observation array design is clear.

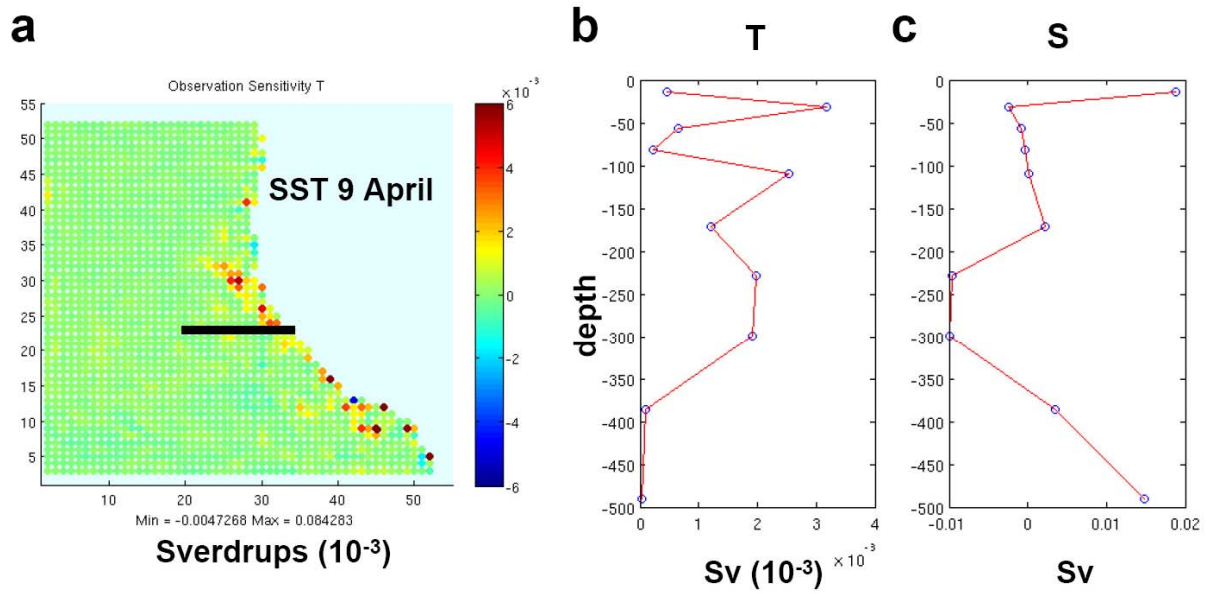


Figure 6: (a) A map of the contribution of each satellite SST observation on 9 April to the total analysis increment CCS transport along 37N on 11 April. Each colored circle represents the location of a single observation. (b) The contribution of subsurface temperature observations to the total analysis increment transport versus depth for a single CalCOFI Line 90 CTD cast. (c) Same as (b) but for salinity observations from the same CTD cast. The black line in (a) indicates the location of the analysis increment transport section.

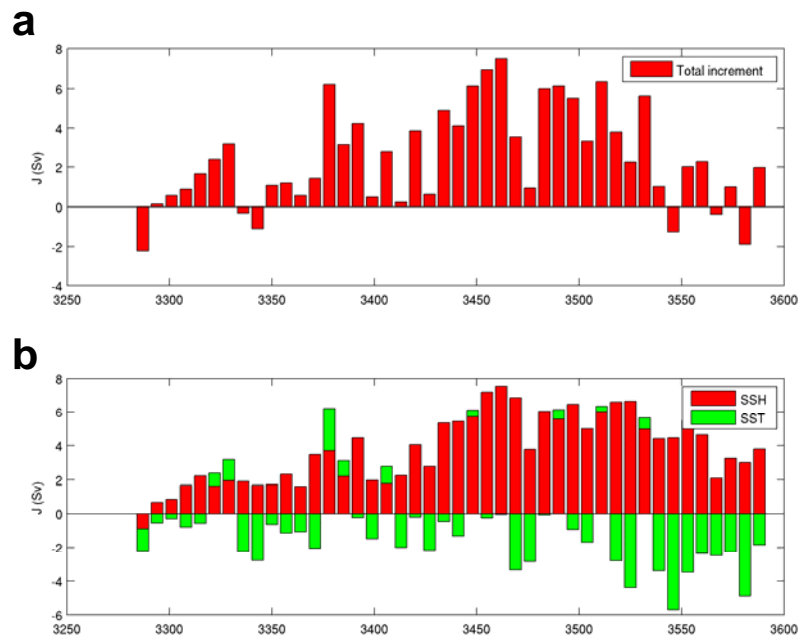


Figure 7: (a) A time series of the increment in the 7 day average Yucatan transport (i.e. transport of the analysis minus transport of the background) for each 7 day assimilation cycle during 1999. (b) A time series of the contribution of satellite SSH and SST observations to the analysis increment transport for each cycle.

Intra Americas Sea (IAS)

Observation impact calculations are currently underway using the new and improved configuration of ROMS IAS. Figures 7 and 8 show some example calculations for the R4D-Var experiment described above where satellite SST and SSH observations were sequentially assimilated into ROMS IAS every 7 days using R4D-Var. Figure 7a shows a time series of the difference in 7 day average Yucatan Channel transport between the analysis circulation and the background circulation. This will be referred to as the Yucatan transport increment. The average Yucatan transport of the analysis during 1999 was ~ 24 Sv, and the analysis increments arising from data assimilation are generally positive indicating that the Yucatan Channel transport is typically stronger during the R4D-Var analysis. Figure 7b shows a similar time series, but now indicates the contribution to the Yucatan transport increment due to SSH and SST observations during each R4D-Var data assimilation cycle. The sum of the red and green bars in Fig. 7b equals the net transport increment shown in Fig. 7a. Notice how the SSH observations tend to strengthen the Yucatan transport of the analysis, while the SST observations generally act to decrease the transport.

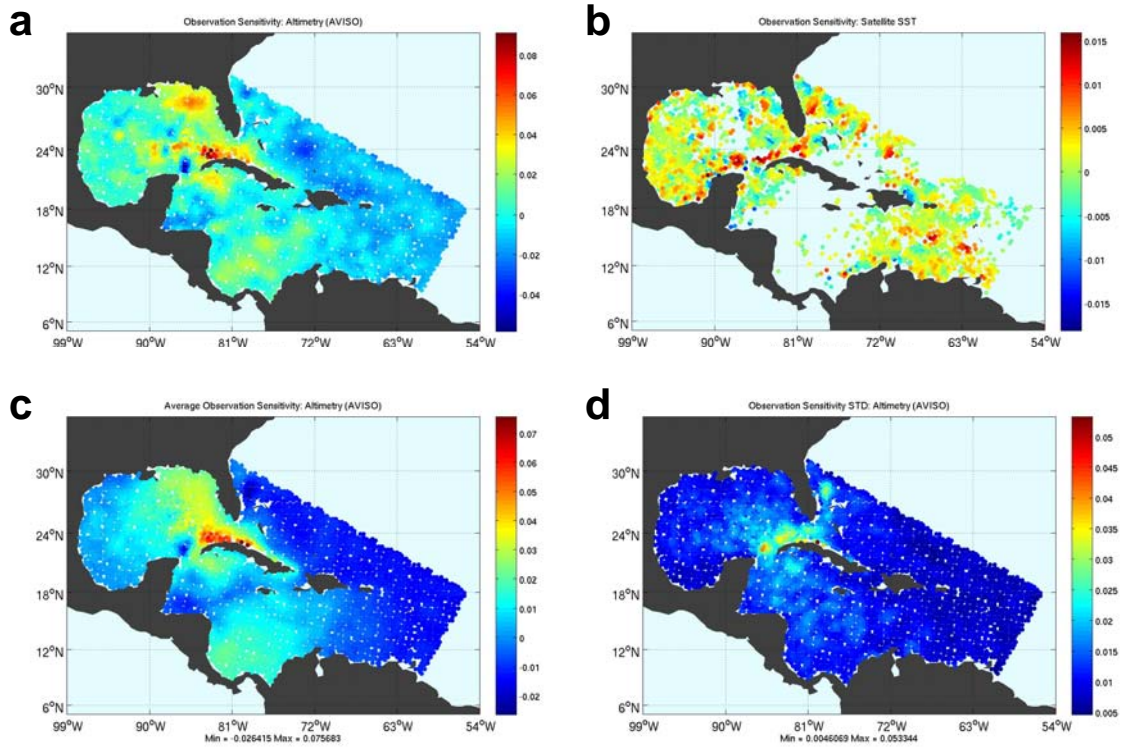


Figure 8: (a) The contribution of each SSH observation to the 7 day average Yucatan transport increment during a representative 7 day assimilation cycle using R4D-Var. (b) Same as (a) but for SST. (c) The average contribution of SSH to the 7 day Yucatan transport for all assimilation cycles during 1999. (d) The standard deviation of the contribution of SSH to the 7 day Yucatan transport about the mean in (c). All units in the color bars are in Sverdrups.

Figures 8a and 8b shows examples of the impact of individual SST and SSH observations on the Yucatan transport increment during a typical 7 data assimilation cycle. During this particular

cycle, SSH observations north of Cuba and on the west Florida shelf exert the largest positive influence on the Yucatan Channel transport, while there are regions of significant negative influence in the Channel itself and north of the Windward Passage. In the case of SSH observations, a gridded product from AVISO was assimilated into the model meaning that the SSH observations when available are always present at the same geographic locations. In this case it is possible to compute the time mean and standard deviation of the contribution of observations at each SSH grid location to the 7 day average Yucatan transport as shown in Figs. 8c and 8d. Figure 8c indicates that SSH observations along the north of Cuba and within the Loop Current extension typically exert the largest positive influence on the Yucatan transport increment during 1999. The standard deviations of Fig. 8d indicate significant variability in SSH impact on Yucatan transport, but mainly confined to the path of the Florida Current.

(c) Multimodel Ensemble Methods

Krishnamurti et al. (2000) have proposed a straightforward and highly effective method for constructing multimodel ensembles based on a linear regression technique. In summary, the value of any gridpoint variable S in the multimodel superensemble is given by

$$S = \bar{O} + \sum_{i=1}^N a_i (F_i - \bar{F}_i),$$

where F_i denotes the gridpoint value corresponding the i^{th} ensemble

member, O denotes the observed value of the variable under consideration, and an overbar denotes the time mean. The ensemble size is N , and the regression coefficients a_i are determined

by minimizing $G = \sum_{t=1}^M (S_t - O_t)^2$, where $t=[1,M]$ represents a training period, and S_t and O_t are

the superensemble and observed gridpoint variables respectively at time t . In general, there will be a different set of regression coefficients a_i for each gridpoint, for each variable, and each forecast lead time.

Jo Beck, a first year graduate student supervised by Andrew Moore, has been working to implement the Krishnamurti superensemble method using ROMS IAS. As an initial test of the method, a 4 member model ensemble was constructed using different combinations of surface forcing (NCEP reanalysis vs ECMWF reanalysis vs NCEP CORE) and different open boundary conditions (SODA vs a ROMS full N. Atlantic solution). One member was chosen as a surrogate for the truth, and the upper 500m ocean temperature and salinity were sampled at every grid point every 3 days during a 1997 training period and assimilated into the other three versions of ROMS using I4D-Var. At the end of each 3 day assimilation cycle a 7 day forecast was initiated and the skill of the forecast in recovering the true solution was computed. Figure 9 shows the average rms error in SST during the training period of each of the three models as a function of forecast lead time for a representative location in the central Gulf of Mexico. Also shown in Fig. 9 is the rms error of the SST superensemble computed using the Krishnamurti method. Clearly the average skill of the superensemble is superior to the majority of individual ensemble member at most forecast lead times, demonstrating the effectiveness and utility of the method.

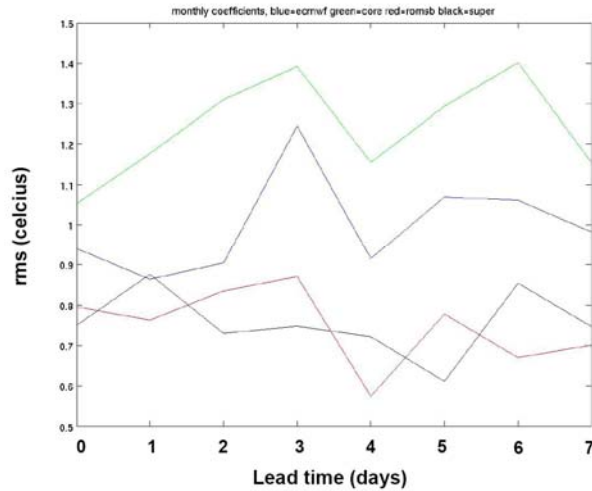


Figure 9: Time series of the average rms error in SST at a location in the central Gulf of Mexico versus forecast lead time for three members of a ROMS model ensemble (blue, green and red curves). The black curve shows the corresponding average rms error for a superensemble for SST at the same location. The average rms was computed from a sequence of 3 day assimilation cycles and forecasts run each week during the 1997 training period.

PLANS FOR THE REMAINING PROJECT PERIOD

As noted in the Approach section, the utility of ROMS 4D-Var has increased considerably during the last 6 months or so, and this project will capitalize on these developments during the remainder of the project period. The preliminary sequence of R4D-Var assimilation experiments during 1999 and described above using ROMS IAS will be extended to 2006 taking account for uncertainties in the initial conditions, surface forcing, and open boundary conditions. For each assimilation cycle, the leading EOFs of \mathbf{E}^a will be computed, and the general characteristics of the expected analysis error that is captured by the EOFs will be explored, including seasonal variations, circulation regime dependences, etc. Observation impact and observation sensitivity studies will also be conducted on the back-end of each assimilation cycle for specific features of the circulation, such as Yucatan Channel transport, Loop Current extent, etc. We are particularly interested in assessing the impact of subsurface ADCP observations that were collected during the *Explorer of the Seas* program.

Development of the multi-model super ensemble technique will continue with plans to apply it to various available ocean reanalysis products.

IMPACT/APPLICATIONS

This project contributes significantly to the functionality and utility of the Regional Ocean Modeling System (ROMS), a popular and important community model and resource. ROMS is in fact unique in that of all the community ocean models that are available, ROMS is the only model that possesses such a wide range of 4D-Var algorithms, analysis tools, and diagnostic capabilities. The posterior analysis error EOF, observation impact and sensitivity, and multi-model super ensemble tools that are being developed as a part of this project have advanced ROMS to a state where it is comparable to the most sophisticated operational systems currently available at several premier numerical weather prediction centers worldwide.

TRANSITIONS

The new ROMS utilities developed as part of this project are available from the ROMS web site and will be actively used and further developed by other research groups in the U.S. and elsewhere as user competence increases. Training sessions and workshops are planned for Spring and Summer 2009 at both the University of Hawaii, and at the University of California to help experienced ROMS users transition to the 4D-Var systems.

RELATED PROJECTS

The work described here is closely related to the following ONR supported projects:

“A community Terrain-Following Ocean Model (ROMS)”, PI Hernan Arango, grant number N00014-08-1-0542.

“Bayesian Hierarchical Models to Augment the Mediterranean Forecast System”, PI Ralph Miliff, grant number N00014-05-C-0198.

REFERENCES

Bennett, A.F., 1985: Array design by inverse methods. *Prog. Oceanogr.*, **15**, 129-156.

Broquet, G., C.A. Edwards, A.M. Moore, B.S. Powell, M. Veneziani and J.D. Doyle, 2009a: Application of 4D-Variational data assimilation to the California Current System. *Dyn. Atmos. Oceans*, **47**, doi:10.1016/j.dynatmoce.2009.03.001.

Broquet, G., A.M. Moore, H.G. Arango, C.A. Edwards and B.S. Powell, 2009b: Ocean state and surface forcing correction using the ROMS-IS4DVAR data assimilation system. *MERCATOR Newsletter*, **34**, 5-13.

Broquet, G., A.M. Moore, H.G. Arango and C.A. Edwards, 2009c: Corrections to ocean surface forcing in the California Current system using 4D variational data assimilation. *Ocean Modelling*, Submitted.

Courtier, P., 1997: Dual formulation of four-dimensional variational assimilation. *Q. J. R. Meteorol. Soc.*, **123**, 2449-2461.

Courtier, P., J.-N. Thépaut and A. Hollingsworth, 1994: A strategy for operational implementation of 4D-Var using an incremental approach. *Q. J. R. Meteorol. Soc.*, **120**, 1367-1388.

Da Silva, A., J. Pfaendtner, J. Guo, M. Sienkiewicz and S. Cohn, 1995: Assessing the effects of data selection with DAO's physical-space statistical analysis system. Proceedings of the second international WMO symposium on assimilation of observations in meteorology and

oceanography, Tokyo 13-17 March, 1995. WMO.TD 651, 273-278.

Di Lorenzo, E., A.M. Moore, H.G. Arango, B.D. Cornuelle, A.J. Miller, B. Powell, B.S. Chua and A.F. Bennett, 2007: Weak and strong constraint data assimilation in the inverse regional ocean modeling system (ROMS): development and application for a baroclinic coastal upwelling system. *Ocean Modelling*, **16**, 160-187.

Egbert, G.D., A.F. Bennett and M.C.G. Foreman, 1994: TOPEX/POSEIDON tides estimated using a global inverse method. *J. Geophys. Res.*, **99**, 24,821-24,852.

Langland, R.H. and N. Baker, 2004: Estimation of observation impact using the NRL atmospheric variational data assimilation adjoint system. *Tellus*, **56A**, 189-201.

Moore, A.M., H.G. Arango, G. Broquet, B.S. Powell, J. Zavala-Garay and A.T. Weaver, 2009a: The Regional Ocean Modeling System (ROMS) 4-dimensional variational data assimilation systems. Part I: Formulation. *Ocean Modelling*, In preparation.

Moore, A.M., H.G. Arango, G. Broquet, M. Veneziani, C.A. Edwards and B.S. Powell, 2009a: The Regional Ocean Modeling System (ROMS) 4-dimensional variational data assimilation systems. Part II: Performance and Application to the California Current System. *Ocean Modelling*, In preparation.

Powell, B.S., H.G. Arango, A.M. Moore, E. Di Lorenzo, R.F. Milliff and D. Foley, 2008: 4DVAR Data Assimilation in the Intra-Americas Sea with the Regional Ocean Modeling System (ROMS). *Ocean Modelling*, **23**, 130-145.

Powell, B.S., A.M. Moore, H.G. Arango, E. Di Lorenzo, R.F. Milliff and R.R. Leben, 2009: Near real-time assimilation and prediction in the Intra-Americas Sea with the Regional Ocean Modeling System (ROMS). *Dyn. Atmos. Oceans*, In press.

Powell, B.S. and A.M. Moore, 2009: Estimating the 4DVAR analysis error from GODAE products. *Ocean Dynamics*, **59**, 121-138.

Zhu, Y. and R. Gelaro, 2008: Observation sensitivity calculations using the adjoint of the Gridpoint Statistical Interpolation (GSI) analysis system. *Mon. Wea. Rev.*, **136**, 335-351.

PUBLICATIONS

Broquet, G., A.M. Moore, H.G. Arango, C.A. Edwards and B.S. Powell, 2009b: Ocean state and surface forcing correction using the ROMS-IS4DVAR data assimilation system. *MERCATOR Newsletter*, **34**, 5-13.

Broquet, G., A.M. Moore, H.G. Arango and C.A. Edwards, 2009c: Corrections to ocean surface forcing in the California Current system using 4D variational data assimilation. *Ocean Modelling*, Submitted.

Moore, A.M., H.G. Arango, G. Broquet, B.S. Powell, J. Zavala-Garay and A.T. Weaver, 2009a: The Regional Ocean Modeling System (ROMS) 4-dimensional variational data assimilation systems. Part I: Formulation. *Ocean Modelling*, In preparation.

Moore, A.M., H.G. Arango, G. Broquet, M. Veneziani, C.A. Edwards and B.S. Powell, 2009a: The Regional Ocean Modeling System (ROMS) 4-dimensional variational data assimilation systems. Part II: Performance and Application to the California Current System. *Ocean Modelling*, In preparation.

Powell, B.S. and A.M. Moore, 2009: Estimating the 4DVAR analysis error from GODAE products. *Ocean Dynamics*, **59**, 121-138.